19

The influence of band structure anisotropy on the plasma oscillations propagation along a conductive nanolayer

© O.V. Savenko

Demidov State University, Yaroslavl, Russia

e-mail: savenko.oleg92@mail.ru Received November 15, 2024 Revised February 03, 2025 Accepted June 02, 2025

A theoretical model of surface plasma oscillations propagation in a conductive nanolayer is constructed taking into account the symmetrical charge distribution at the nanolayer boundaries. It is assumed that the conductor constant energy surface is an ellipsoid of revolution. The surface wave frequency is limited from above by the near IR frequency. The nanolayer thickness can be comparable to or smaller than the charge carrier de Broglie wavelength. Surface scattering of charge carriers is taken into account through the Soffer boundary conditions. Analytical expressions are obtained for the wave propagation coefficient, attenuation coefficient, and propagation length. We conducted the analysis of the surface wave characteristics dependences on the dimensionless parameters: the conductive layer thickness, the surface wave frequency, the chemical potential, the insulating layer permittivity, the "semiconductor-dielectric" interfaces roughness parameters, and the isoenergetic surface ellipticity parameter.

Keywords: surface plasmon, conductive nanolayer, kinetic equation, propagation coefficient, propagation length.

DOI: 10.61011/EOS.2025.06.61667.7340-25

Introduction

Currently, research in plasmonics is a rapidly developing There is a transition from traditional electronic integrated circuits to photonic circuits, in which information is transmitted not by electric current but by the flow of photons [1]. Optical fibers and photonic crystals can be used as optical signal transmission elements; however, their characteristic size is limited by the wavelength of the electromagnetic radiation (for the visible range, this size should be no less than hundreds of nanometers). Using plasmonic waveguides can solve the problem, since the plasmon wavelength can be shorter than the wavelength of electromagnetic radiation. Effects associated with a wavelength shorter than that of electromagnetic radiation can be utilized in microscopy to obtain images of objects whose sizes are smaller than the wavelength of electromagnetic radiation. All of the above indicates the relevance of theoretical studies of the features of plasma oscillation propagation in nanostructures. Modern technologies allow the creation of nanolayers with characteristic sizes of several In such nanolayers, surface roughness at the atomic level and size quantization effects of charge carriers significantly influence transport phenomena. For the theoretical description of parameters of surface oscillations propagating along nanolayers, it is necessary to take into account surface scattering of charge carriers and quantization of their energy spectrum.

Among the first scientific works devoted to taking into account surface roughness on the nature of plasma oscillation propagation, the works [2-4] can be noted. Kretschmann, in work [2], used exact solutions of integral equations obtained

from the problem of electromagnetic wave diffraction on a rough surface to investigate the plasmon dispersion law. Surface roughness was accounted for through a Gaussian correlation function. Kretschmann discovered the splitting of the maximum of the frequency dependence of the propagation coefficient due to the presence of roughness. Later, in works [3,4], the Green's function method was employed to account for surface roughness. Among recent publications, works [5–9] an be noted. These works obtained expressions only for optical coefficients, but did not take into account the influence of surface roughness on the frequency dependence of the plasmon wave number.

Currently, widely used semiconductors include silicon and germanium, whose constant energy surfaces are not spherical but consist of several rotational ellipsoids. A relevant problem is the influence of the anisotropy of the isoenergetic surface on the nature of plasmon propagation along silicon and germanium nanolayers. It should be noted that some semimetals (such as bismuth, antimony, etc.) have constant energy surfaces consisting of elongated rotational ellipsoids. Interest in bismuth is due to pronounced manifestation of size quantization effects. Size quantization effects can significantly influence the parameters of the surface wave.

In this work, a theoretical model of surface plasma oscillations in a conducting nanolayer is developed, taking into account quantum transport theory effects, surface scattering of charge carriers, and the ellipsoidal shape of the conductive material's isoenergetic surface. The situation is considered where the conducting nanolayer is located

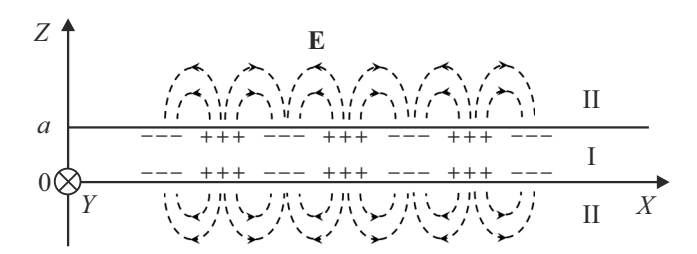


Figure 1. Nanostructure "dielectric—conductor—dielectric" (I conducting layer, II — insulating layer). Dashed lines show the electric field intensity lines.

between two insulating layers with identical dielectric permittivities.

Problem formulation

Consider the nanostructure "dielectric—conductor—dielectric". We assume that the dielectric layers are non-magnetic and have identical dielectric permittivities. The conducting nanolayer can be made from metal or doped semiconductor. A coordinate system is chosen so that the Z axis is directed perpendicular to the plane of the nanostructure, and the Xaxis is parallel to the propagation direction of the surface wave (Fig. 1). The electric and magnetic components of the surface wave are assumed to have the following form:

$$\mathbf{E} = \{E_x, 0, E_z\}, \quad \mathbf{H} = \{0, H_y, 0\}.$$

In this work, it is assumed that the insulating layers are made of non-polar dielectric or wide-bandgap semiconductor with ionic bonding. In this case, the electric field causes only electronic and ionic polarization in the dielectric [10], and the dielectric permittivity can be considered a constant.

In the upper and lower dielectric layers, the components of the electric and magnetic field intensity vectors satisfy Maxwell's equations:

$$\begin{cases} \frac{\partial E_{x}}{\partial z} - ikE_{z} - i\frac{\omega}{c}H_{y} = 0, \\ -i\varepsilon\frac{\omega}{c}E_{z} + ikH_{y} = 0, \\ -\frac{\partial H_{y}}{\partial z} + i\varepsilon\frac{\omega}{c}E_{x} = 0. \end{cases}$$
 (1)

Here, ω is the frequency of the surface wave, k is the wave number, ε — is the dielectric permittivity of the insulating layers, and c — is the speed of light.

Substituting the conductivity (1) $\varepsilon = 1 + i4\pi\sigma/\omega$, where ε — into the system of equations, we obtain the relation between components of the vectors E and H inside the conducting layer.

The solution of Maxwell's equations can be written as a wave propagating along the X axis and decaying in the direction perpendicular to the plane of the conducting nanolayer:

$$\begin{cases} \mathbf{E} = \mathbf{E}_{0} \exp(-i\omega t + \alpha z + ikx), & z < 0, \\ \mathbf{E} = \mathbf{E}_{0} \exp(-i\omega t + \alpha(a - z) + ikx), & z > a, \end{cases}$$
(2)
$$\begin{cases} \mathbf{H} = \mathbf{H}_{0} \exp(-i\omega t + \alpha z + ikx), & z < 0, \\ \mathbf{H} = \mathbf{H}_{0} \exp(-i\omega t + \alpha(a - z) + ikx), & z > a. \end{cases}$$
(3)

$$\begin{cases}
\mathbf{H} = \mathbf{H}_0 \exp(-i\omega t + \alpha z + ikx), & z < 0, \\
\mathbf{H} = \mathbf{H}_0 \exp(-i\omega t + \alpha(a - z) + ikx), & z > a.
\end{cases} \tag{3}$$

Here, α the transverse coefficient of decay that is determined via the parameters k, ω and ε by the relation:

$$\alpha = \sqrt{k^2 - \frac{\omega^2}{c^2} \varepsilon}.$$
 (4)

It is assumed that the surface wave frequency is less than the plasma resonance frequency. The case of symmetric distribution of charge carriers at the boundaries of the conducting layer (Fig. 1) is considered. This situation is characterized by the following relation between components of the vectors **E** and **H**:

$$\begin{cases} H_{y}(0) = -H_{y}(a), \\ E_{z}(0) = -E_{z}(a), \\ E_{x}(0) = E_{x}(a). \end{cases}$$
 (5)

In this work, the conducting nanolayer is considered sufficiently thin so that components of the electric field vector E_x slightly vary within it. The thickness of the nanolayer may be comparable to or less than the de Broglie wavelength of the charge carriers. In this situation, the charge carrier system must be considered quantum. The electron gas shall be reviewed as a quasi-two-dimensional gas included in a quantum well with infinitely high walls. It is assumed that the isoenergetic surface is an ellipsoid with principal axes directed parallel to the X, Y and Zaxes.

The expression for the total energy of a charge carrier in the 1-th subband is:

$$\varepsilon_{l} = \frac{\hbar^{2}}{2m_{1}}k_{x}^{2} + \frac{\hbar^{2}}{2m_{2}}k_{y}^{2} + \varepsilon_{zl}, \tag{6}$$

$$\varepsilon_{zl} = \frac{(\pi\hbar l)^2}{2m_3 a^2},\tag{7}$$

where \hbar — Planck constant, ε_{zl} — eigenvalue of the charge carrier in the l-th subband, the index l takes values from 1 to N (N is the total number of subbands), m_1 , m_2 and m_3 are the effective masses of the charge carriers along the X, Y and Zaxes, respectively.

According to quantum transport theory, the charge carrier system is described by the density operator: [11]:

$$\hat{\rho}(z, \mathbf{k}_{\parallel}, t) = \sum_{l} W_{l} |\psi_{l}(z, \mathbf{k}_{\parallel}, t)\rangle \langle \psi_{l}(z, \mathbf{k}_{\parallel}, t)|, \quad (8)$$

which satisfies the quantum Liouville equation:

$$i\hbar\frac{\partial\hat{\rho}}{\partial t} = \left[\hat{H},\hat{\rho}\right],\tag{9}$$

where ψ_l is the wave function of the charge carrier system in the l-th subband, W_l is the statistical weight, and \mathbf{k}_{\parallel} is the longitudinal component of the wave vector.

In the case of small deviation of the charge carrier system from equilibrium, the problem of finding the density operator can be solved within perturbation theory. In this situation, the Hamiltonian can be written as follows [12]:

$$\hat{H} = \hat{H}_0 + \hat{V},\tag{10}$$

where \hat{H}_0 — is the equilibrium Hamiltonian, and V is the perturbation accounting for bulk and surface scattering.

Note that in some semiconductors, the dependence of the equilibrium Hamiltonian on the wave number may significantly differ from the quadratic law. For example, in *p*-type semiconductors, spin-orbit interaction greatly affects the system's Hamiltonian [13]. The ellipsoidal dispersion law considered in this work applies to electrons in the conduction band.

It is assumed that the material of the nanolayer is a metal or n-type semiconductor in which the equilibrium Hamiltonian \hat{H}_0 of the charge carrier system in the conduction band depends quadratically on the wave number.

Equation (9) can be reduced to the following kinetic equation for the distribution function of charge carriers in the *l*-th subband f_l , which plays the role of the diagonal element of the density matrix ρ_{ll} [12,14]:

$$-i\omega f_l + \frac{\hbar k_{zl}}{m_3} \frac{\partial f_l}{\partial z} + \frac{e\mathbf{E}}{\hbar} \frac{\partial f_l}{\partial \mathbf{k}_{\parallel}} = -\frac{f_l - f_l^0}{\tau},\tag{11}$$

$$k_{zl} = \pi \hbar l/a. \tag{12}$$

Here τ is the relaxation time, \hbar is the Planck constant, k_{zl} is the perpendicular component of the charge carrier velocity vector in the l-th subband, and, e is the electron (hole) charge. The kinetic equation (11) involves the components of the distribution function f_l^0 and $f_l^{(1)}$, which enter the expansion of f_l linear in the external field:

$$f_l(z, \mathbf{k}_{\parallel}, t) = f_l^{(0)} + f_l^{(1)}(z, \mathbf{k}_{\parallel}) \exp(-i\omega t),$$
 (13)

$$f_l^{(0)} = \frac{1}{1 + \exp((\varepsilon_l - \mu)/k_{\rm B}T)},$$
 (14)

where $f_l^{(0)}$ is the equilibrium distribution function, $f_l^{(1)}$ is the nonequilibrium correction, μ is the chemical potential, $k_{\rm B}$ is the Boltzmann constant, and T is temperature.

The relaxation time is considered as a diagonal secondrank tensor:

$$\tau = \begin{pmatrix} \tau_1 & 0 & 0 \\ 0 & \tau_2 & 0 \\ 0 & 0 & \tau_3 \end{pmatrix}. \tag{15}$$

Surface scattering of charge carriers is taken into account through Soffer boundary conditions [15], imposed on equation (11):

$$\begin{cases}
f_l^{(1)+} = q_1(g_1, \theta) f_l^{(1)-} & \text{if } z = 0, \\
f_l^{(1)-} = q_2(g_2, \theta) f_l^{(1)+} & \text{if } z = a,
\end{cases}$$
(16)

$$q_{1,2}(g_{1,2},\theta) = \exp(-(4\pi g_{1,2}\cos\theta)^2),$$
 (17)

$$g_{1,2} = \frac{g_{s1,2}}{\lambda_{\rm B}},\tag{18}$$

where $f_l^{(1)+}$ and $f_l^{(1)-}$ are corrections to the distribution functions of the charge carriers with positive and negative projections of the wave vector on the Zaxis, respectively; $g_{s1,2}$ is the root-mean-square height of the surface roughness of the upper and lower surfaces; $\lambda_{\rm B}$ is the de Broglie wavelength of the charge carrier; θ is the angle of incidence of the charge carrier on the internal surface of the conducting nanolayer.

The author of [15] questioned the applicability of this boundary condition model to semimetals and semiconductors due to the failure of the far-field approximation used to compute the amplitude of the scattered de Broglie wave at the nanolayer boundary. We will show that Soffer's model can be used for semiconductors. The charge carrier system in metals and semiconductors can be considered as a collection of wave packets formed by the interference The far-field approximation can be of Bloch waves. satisfied due to the small size of the wave packet [15]. In semiconductors, phonon and impurity scattering may change the amplitude of the wave vector (de Broglie wavelength), i.e., there is a distribution of thermal velocities of charge carriers. This is an additional factor that affects the smallness of the wave packet and ensures the validity of the far-field approximation.

The kinetic equation (11) was derived within perturbation theory, which limits the allowable values of the root-mean-square surface roughness height. In this work, it is assumed that the quantity $g_{s1,2}$ is much smaller than the thickness of the nanolayer. This assumption leads to parameters g_{s1} and g_{s2} being less than the de Broglie wavelength $\lambda_{\rm B}$ of charge carriers in the case when the nanolayer thickness is comparable to $\lambda_{\rm B}$, which corresponds to the condition for which the far-field approximation is valid: [16]:

$$\frac{g_{s1,2}^2}{b\lambda_{\rm R}} \ll 1,\tag{19}$$

where b is a characteristic scale of the de Broglie wave amplitude variation.

The nonequilibrium distribution function allows calculation of the current density and integral conductivity by the formulas: [12,14]:

$$j_x = \frac{2ek_{z1}}{(2\pi)^3} \sum_{l} \iint v_x \left(f_l^{(1)} + f_l^{(1)-} \right) dk_x dk_y, \qquad (20)$$

$$\sigma = \int_{0}^{a} \frac{j_x}{E_x} dz. \tag{21}$$

Characteristics of the Surface Wave

After performing a series of mathematical calculations (Appendix), the following expressions are obtained for the parameters of the surface wave k and α , normalized by the nanolayer thickness:

$$\alpha a = -\frac{2\varepsilon y_0}{(y_0 + iy_p^2 \Sigma)},\tag{22}$$

$$ka = \sqrt{y_0^2 \frac{x_0^2}{x_{\lambda}^2} \rho^2 \varepsilon + \frac{4y_0^2 \varepsilon^2}{(y_0 + iy_p^2 \Sigma)^2}}.$$
 (23)

Here Σ is the dimensionless conductivity of the nanolayer, x_0 is the dimensionless thickness, x_λ is the dimensionless mean free path of charge carriers, y_0 is the dimensionless frequency of the surface wave, y_p is the dimensionless plasma frequency, and ρ is the ratio of the characteristic velocity of the charge carriers to the speed of light.

Note that, in general, the parameters α and k are complex quantities, i.e., one can write:

$$\alpha = \operatorname{Re}(\alpha) + i\operatorname{Im}(\alpha) = \alpha_1 + i\alpha_2,$$
 (24)

$$k = \text{Re}(k) + i\text{Im}(k) = k_1 + ik_2.$$
 (25)

The real part of k characterizes the wave number, which we will call the propagation constant. The imaginary part of k describes the attenuation of the surface wave along the propagation direction; we call it the longitudinal attenuation coefficient. The real part of α describes the attenuation of the surface wave in the direction of the Z axis; this parameter will be called the transverse attenuation coefficient.

From a practical point of view, it is of interest to determine the parameter characterizing the distance over which the amplitude of the surface wave decreases by a factor of e due to attenuation (propagation length). From expressions (2) and (3), it follows that the propagation length is the reciprocal of the imaginary part of the wave number k. Normalizing by the thickness of the conducting nanolayer, we get:

$$\frac{L}{a} = \frac{1}{\text{Im}(ka)}. (26)$$

Most often, the case is realized where the constant energy surface of semiconductors is a spheroid. For example, the constant energy surface of silicon consists of six ellipsoids, and that of germanium consists of eight ellipsoids. In the analysis of results, we consider the situation where two principal axes of the triaxial ellipsoid are equal. We examine three options for the orientation of the ellipsoid's rotational axis: the axis is directed along the X axis (longitudinal orientation), along the Y axis (transverse orientation), and along the Z axis (perpendicular orientation).

In the case when the principal axis of the ellipsoidal constant energy surface is directed at an arbitrary angle relative to the wave propagation direction, the problem of finding the characteristics of plasma oscillations can be reduced to

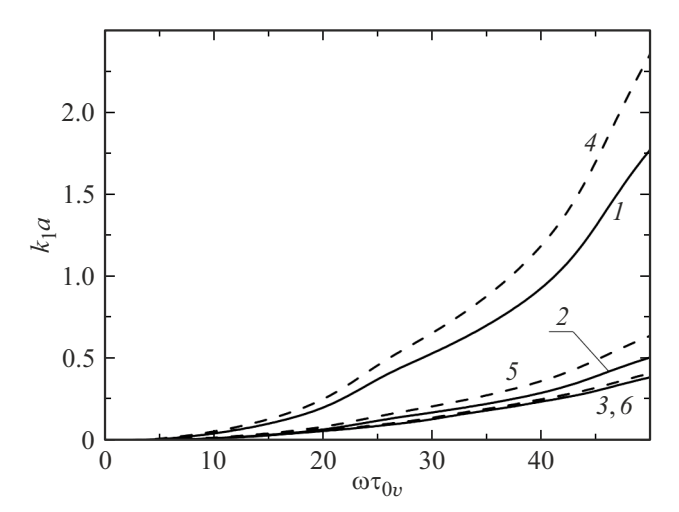


Figure 2. Dependencies of the propagation coefficient k_1 , normalized by layer thickness, on the dimensionless frequency $\omega \tau_{0v}$ for $a/\lambda_{B0}=1$, $\Lambda/\lambda_{B0}=10$, $\varepsilon=3$, $v_{0v}/c=0.005$, $\omega_p\tau_{0v}=200$, $g_1=0$, $g_2=0.2$, $m_\perp/m_0=0.7$. Solid curves I-3 and dashed curves 4-6 are plotted for degenerate and non-degenerate electron gas respectively. The curves correspond to the following orientation options of the constant energy ellipsoid principal axis I and I-10 and I-11 and I-12 and I-13 and I-13 and I-14 and I-13 and I-14 and I-14 and I-15 and I-15

the situation when the principal axis is aligned with the axes X and Y, by decomposing the components of the electric and magnetic field intensity vectors. The resulting plasma oscillations can be represented as a superposition of surface plasma oscillations propagating along the axes X and Y. In the case of multivalley semiconductors (silicon, germanium, etc.), plasma oscillations can be represented as a superposition of oscillations of charge carriers located in each spheroid.

Analysis of results

For numerical analysis of surface wave characteristics, Figures 2 and 3 show results for parameters corresponding to an n-type silicon nanolayer with carrier concentration $10^{18} \,\mathrm{cm}^{-3}$. The corresponding dimensionless parameters are $\gamma = 0.7$, $\rho = 0.005$, $y_p = 200$ (γ is the ellipticity parameter, defined as the ratio of the transverse effective mass to the scalar mass m_0). this situation, at room temperature, the electron gas can be considered non-degenerate. To compare under the same dimensionless parameters with the degenerate electron gas case (without changing the carrier concentration), the temperature is changed. The free path of charge carriers ignoring surface scattering, included in the plasma frequency y_p , does not change significantly since in a sufficiently thin layer this parameter is determined by scattering on impurities and lattice defects.

Figure 2 shows the dependence of the propagation coefficient normalized by layer thickness on the dimen-

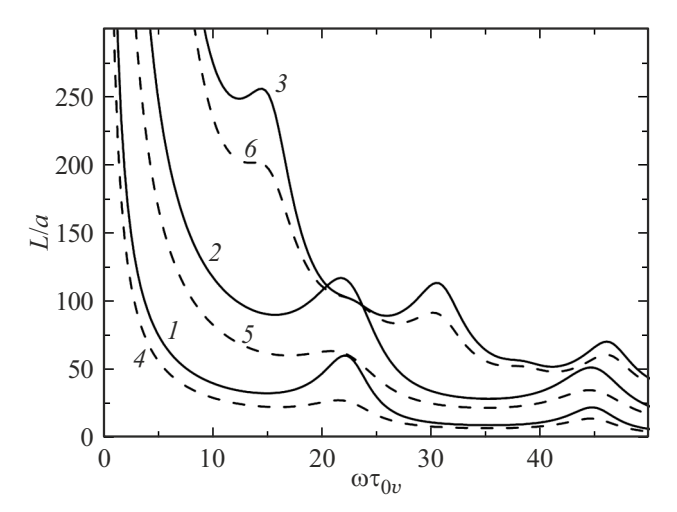


Figure 3. Dependencies of the propagation length L, normalized by the layer thickness, on the dimensionless frequency $\omega\tau_{0v}$ at $a/\lambda_{B0}=1$, $\Lambda/\lambda_{B0}=10$, $\varepsilon=3$, $v_{0v}/c=0.005$, $\omega_p\tau_{0v}=200$, $g_1=0$, $g_2=0.2$, $m_\perp/m_0=0.7$. Solid curves I-3 and dashed curves 4-6 are plotted for degenerate and non-degenerate electron gas respectively. The curves correspond to the following orientation options of the constant energy ellipsoid principal axis: I and I longitudinal, I lo

sionless frequency of the surface wave for the longitudinal, transverse, and perpendicular orientations of the principal axis of the constant energy ellipsoid. The highest coefficient k_1 is observed in the first case (curves 1 and 4). This is possibly due to the large longitudinal effective mass of charge carriers compared to the transverse mass for an elongated ellipsoid. The difference between curves 2 and 3 (5 and 6) is small and can be explained by differing influence of surface scattering of charge carriers on the propagation coefficient k_1 . In the case when the principal axis of the ellipsoid is perpendicular to the nanolayer surface (curves 3, 6), the effective mass of charge carriers in the direction parallel to the nanolayer plane is less than in the perpendicular direction. Charge carriers predominantly move in the longitudinal direction, leading to an increase in the region of excess charge in the surface wave, i.e., a decrease in wave number. The figure shows that the propagation coefficient in the case of a non-degenerate electron gas is larger than in the case of a degenerate gas, which is possibly related to the spread of thermal velocities of the charge carriers.

Figures 3 and 4 show the frequency dependencies of the surface wave propagation length normalized by the thickness of the semiconductor nanolayer. The ellipticity parameter of the constant energy surface equals 0.7 (Fig. 3) and 0.5 (Fig. 4). Oscillations in the propagation length spectra are observed, whose period depends on the orientation of the principal axis of the constant energy ellipsoid. These oscillations arise when the frequency of surface scattering of charge carriers is a multiple of the frequencies of the electric and magnetic field oscillations of the surface wave. A possible reason for the oscillations is

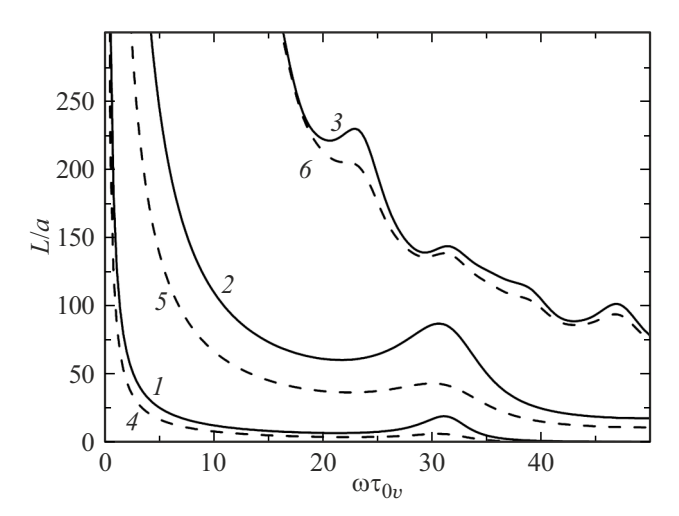


Figure 4. Dependencies of the propagation length L, normalized by the layer thickness, on the dimensionless frequency $\omega \tau_{0v}$ at $a/\lambda_{B0}=1$, $\Lambda/\lambda_{B0}=10$, $\varepsilon=3$, $v_0v/c=0.005$, $\omega_p\tau_{0v}=200$, $g_1=0$, $g_2=0.2$, $m_\perp/m_0=0.5$. Solid curves I-3 and dashed curves 4-6 are plotted for degenerate and non-degenerate electron gas respectively. The curves correspond to the following orientation options of the constant energy ellipsoid principal axis: I and I0 and I1 and I2 and I3 and I4 more perpendicular.

similar to that which causes oscillations in the absorption spectra discovered in [17]. In the cases of longitudinal and transverse orientations, the oscillation period and the position of maxima in the propagation length coincide. This is possibly related to the fact that the effective mass of charge carriers in the direction perpendicular to the nanolayer plane will be the same. Consequently, in the situations described by curves 1 and 2 (3 and 4), the frequency of surface scattering of charge carriers will be the same.

In the case of perpendicular orientation, the effective mass of charge carriers differs from those in the longitudinal and transverse orientations, which influences the change in the oscillation period. Due to the spread of thermal velocities of charge carriers, the oscillation maxima of the propagation length are less pronounced in the non-degenerate gas case than in the degenerate one. The figures also show that plasma oscillations propagate with the least attenuation when the rotation axis of the constant energy ellipsoid is oriented perpendicular to the nanolayer plane. For a silicon nanolayer 10 nm thick and perpendicular orientation of the ellipsoid rotation axis, the propagation length of plasma oscillations at frequencies on the order of 10 THz can reach several micrometers.

Effects related to oscillations in the frequency dependencies of the propagation length can be used to create thin-film plasmonic waveguides that filter frequencies corresponding to minimum attenuation (maxima of the parameter *L*).

Figures 3 and 4 show that the propagation length of the wave increases without bound as frequency decreases. This may indicate the limits of applicability of the theoretical

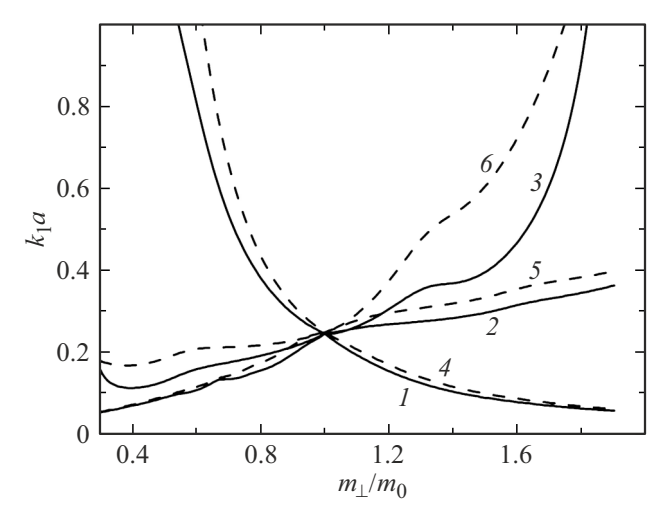


Figure 5. Dependence of the propagation coefficient k_1 , normalized by the layer thickness on the ellipticity parameter m_{\perp}/m_0 for $a/\lambda_{B0}=1$, $\Lambda/\lambda_{B0}=10$, $\omega\tau_{0v}=30$, $\varepsilon=3$, $v_{0v}/c=0.005$, $\omega_p\tau_{0v}=200$, $g_1=0$, $g_2=0.2$. Solid curves I-3 and dashed curves 4-6 correspond to degenerate and non-degenerate electron gas cases, respectively. The curves correspond to the following orientation options of the constant energy ellipsoid principal axis: I and I; longitudinal, I and I; transverse, I and I0 perpendicular.

model developed in this work. As shown in Fig. 2, at the low-frequency limit the parameter k_1 tends to zero. The decrease of the propagation coefficient with decreasing frequency leads to an unlimited increase in the size of surface regions where positive (negative) charge accumulates. This work does not consider effects related to limitations on the size of these regions due to thermal fluctuations of charge carriers. In typical semiconductors, the diffusion length of charge carriers can range from tens to thousands of micrometers. The theoretical model developed here is applicable when the parameter L is much smaller than the diffusion length, i.e., does not exceed about ten micrometers.

Figure 5 shows the dependence of the surface wave propagation coefficient on the ellipticity parameter of the constant energy surface. The figure demonstrates that with increasing ellipticity parameter m_{\perp}/m_0 the propagation coefficient increases for the longitudinal orientation of the main axis of the ellipsoid, while it decreases in the transverse and perpendicular orientations. All curves converge at one point when $m_{\perp}/m_0=1$ corresponding to a spherically symmetric energy band.

Figure 6 shows the dependence of the propagation length on the ellipticity parameter of the constant energy surface. The figure shows that when the principal axis of the constant energy ellipsoid is aligned with the direction of surface wave propagation, the dimensionless propagation length increases with increasing ellipticity parameter; in other cases, it decreases. The dependence $L(m_{\perp}/m_0)$ has a pronounced oscillatory character. The most distinctive oscillations occur for an elongated rotational ellipsoid $(m_{\perp}/m_0 < 1)$ and

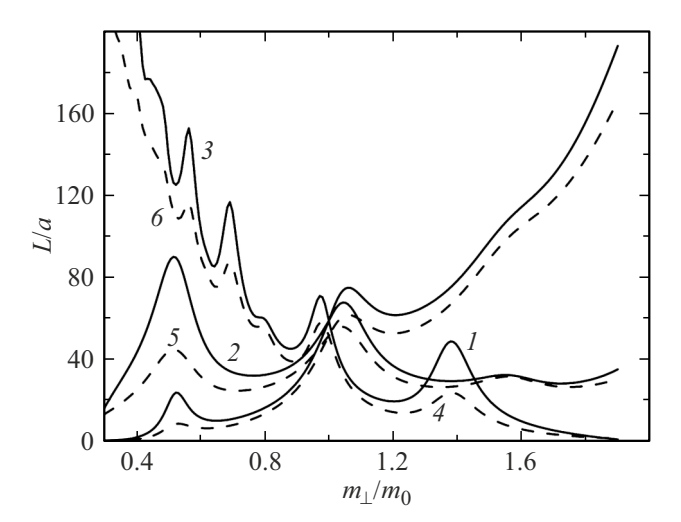


Figure 6. Dependence of the surface wave propagation length L, normalized by the layer thickness, on the ellipticity parameter m_{\perp}/m_0 at $a/\lambda_{B0}=1$, $\Lambda/\lambda_{B0}=10$, $\omega\tau_{0v}=30$, $\varepsilon=3$, $v_{0v}/c=0.005$, $\omega_p\tau_{0v}=200$, $g_1=0$, $g_2=0.2$. Solid curves I-3 and dashed curves 4-6 correspond to degenerate and non-degenerate electron gas cases, respectively. The curves correspond to the following orientation options of the constant energy ellipsoid principal axis: I and I—longitudinal, I and I—transverse, I and I—perpendicular.

perpendicular orientation of the principal axis. Note that the constant energy surface in most semiconductors with anisotropic band structures consists of a set of elongated rotational ellipsoids; thus, the case $m_{\perp}/m_0 < 1$ is very common. Using the oscillatory frequency dependence of the propagation length, it is possible to select a semiconductor nanolayer with the appropriate ellipticity parameter for efficient transmission of plasma oscillations with minimal attenuation. Similarly to Fig. 5, all solid and dashed curves converge in the case of a spherical band structure of the semiconductor.

Conclusion

In this work, analytical expressions for the characteristics of surface plasma oscillations taking into account the anisotropy of the conductor's band structure were obtained as functions of dimensionless parameters: thickness of the conducting nanolayer, surface wave frequency, dielectric permittivity of external insulating layers, ellipticity parameter of the constant energy surface, and surface roughness parameters. The influence of the anisotropy of the constant energy surface frequency dependencies of the wave propagation length was found. The most pronounced oscillations are observed in the case of an elongated rotational ellipsoid with the principal axis oriented perpendicular to the nanolayer plane. It was established that the dependence of the propagation length on the ellipticity parameter (semiconductor material) has an oscillatory character.

The obtained results can be used for designing plasmonic waveguides that filter frequencies corresponding to minimal attenuation.

Appendix

The problem of determining nonequilibrium corrections to the distribution function and finding the integral conductivity is solved similarly to [12,14]. By solving the kinetic equation (11) with boundary condition (16), substituting the found distribution function into the current density expression (20), and then into (21), the following expression for the integral conductivity is obtained:

$$\sigma = \sigma_0 \Sigma, \tag{27}$$

$$\sigma_0 = \frac{n_v e^2 \tau_{0v}}{m_0},\tag{28}$$

$$\Sigma = \frac{\sqrt{u_{0v}}}{2x_0 I_{1/2} z_0 \gamma_1 \sqrt{\gamma_3}} \sum_{l=1}^{\infty} \ln(\exp(u_{\mu} - u_{z1} l^2) + 1) \times \left(1 - \chi\left(\frac{2x_0^2 z_0 \gamma_3}{l x_{\lambda}}\right)\right),$$
(29)

$$\chi(p) = \frac{1}{2p} (1 - e^{-p}) \frac{2 - q_1 - q_2 + (q_1 + q_2 - 2q_1q_2)e^{-p}}{1 - q_1q_2e^{-2p}},$$
(30)

$$q_{1,2}(g_{1,2},\theta) = \exp\left(-(2g_{1,2}l/x_0)^2\right).$$
 (31)

The following dimensionless parameters are introduced:

$$z_0 = \nu \tau_{0\nu} = \kappa - i y_0, \quad x_0 = \frac{a}{\lambda_{B0}},$$

$$x_{\lambda} = \frac{\Lambda}{\lambda_{R0}}, \qquad y_0 = \omega \tau_{0v}, \tag{32}$$

$$\kappa = \frac{\tau_{0v}}{\tau_1} = \frac{\sqrt{u_0}}{\sqrt{u_{0v}}} \frac{1}{\sqrt{\gamma_1}},\tag{33}$$

$$I_s = \int_0^\infty \frac{u^s du}{\exp(u - u_\mu) + 1},\tag{34}$$

$$u_0 = \frac{m_0 v_0^2}{2k_B T}, \quad u_{0v} = \frac{m_0 v_0 v^2}{2k_B T},$$

$$u_{z1} = \frac{\hbar^2 k_{z1}^2}{2m_3 k_B T}, \qquad u_{\mu} = \frac{\mu}{k_B T},$$
 (35)

$$m_0 = \sqrt[3]{m_1 m_2 m_3}, \qquad \tau_{0v} = \sqrt[3]{\tau_{1v} \tau_{2v} \tau_{3v}},$$

$$\gamma_1 = \sqrt{\frac{m_1}{m_0}}, \qquad \gamma_3 = \sqrt{\frac{m_3}{m_0}}.$$
(36)

Parameters x_0 , x_λ are normalized by the de Broglie wavelength of charge carriers moving with characteristic velocity $v_{0\nu}$, z_0 . Parameters y_0 are normalized by the scalar relaxation time of charge carriers $\tau_{0\nu}$ ignoring quantization of their energy spectrum. Velocities v_0 and $v_{0\nu}$ are the characteristic speeds of charge carriers with and without

considering quantization of the energy spectrum, introduced as follows:

$$nv_0^2 = 4\left(\frac{m_0}{h}\right)^3 v_1 \frac{5}{3} \sum_{l=1}^{\infty} \iint V_l^2 f_l^{(0)} dv_x dv_y, \tag{37}$$

$$n_v v_{0v}^2 = 2\left(\frac{m_0}{h}\right)^3 \frac{5}{3} \iiint V^2 f_0 d^3 v,$$
 (38)

$$V_l^2 = \frac{m_1 v_x^2 + m_2 v_y^2 + m_3 v_{z1}^2 l^2)}{m_0},$$
 (39)

$$V^{2} = \frac{(m_{1}v_{x}^{2} + m_{2}v_{y}^{2} + m_{3}v_{z}^{2})}{m_{0}},$$
 (40)

$$v_{z1} = \frac{\hbar k_{z1}}{m_2},\tag{41}$$

 n_v and n — are, respectively, the charge carrier concentrations in the macroscopic sample and in the nanolayer [12,14].

Calculating expressions (37) and (38) and moving to dimensionless parameters, we obtain expressions for the parameters u_0 and u_{0v} :

$$u_0 = \frac{5}{3} \frac{K}{P}, \qquad u_{0v} = \frac{5}{3} \frac{I_{3/2}}{I_{1/2}},$$
 (42)

$$K = \sum_{l=1}^{\infty} \int_{u_{-l}l^2}^{\infty} \frac{u du}{\exp(u - u_{\mu}) + 1},$$
 (43)

$$P = \sum_{l=1}^{\infty} \ln(\exp(u_{\mu} - u_{z1}l^2) + 1). \tag{44}$$

In the case of a degenerate electron gas v0 and v_{v0} reduce to the Fermi velocity vF, while for the non-degenerate gas they are on the order of the average thermal velocity of charge carriers:

$$v_{0v}^2 \approx \frac{5k_B T}{m_0},\tag{45}$$

$$v_0^2 \approx \frac{10k_BT}{3m_0} \left(1 + \frac{\sum u_{z1}l^2 \exp(-u_{z1}l^2)}{\sum \exp(-u_{z1}l^2)} \right).$$
 (46)

The relationship between the dimensionless parameters u_{z1} and u_{0v} can be found using the expression for the charge carrier velocity v_{z1} (41) and the wave number k_{z1} (12):

$$\sqrt{\frac{u_{0v}}{v_{z1}}} = \sqrt{\frac{m_0}{m_3}} \frac{v_{0v}}{v_{z1}} = \sqrt{\frac{m_0}{m_3}} \frac{h}{m_0 \lambda_{B0}} \frac{2m_3 a}{h}$$

$$= \sqrt{\frac{m_3}{m_0}} 2x_0 = 2x_0 \sqrt{y_3}.$$
(47)

In the case of degenerate electron gas $(\exp u_{\mu} \gg 1)$ the dimensionless conductivity Σ takes the form:

$$\Sigma = \frac{3}{4x_0 z_0 \gamma_1 \sqrt{\gamma_3}} \sum_{l=1}^{n} \left(1 - \frac{l^2}{4\gamma_3 x_0^2} \right) \times \left(1 - \chi \left(\frac{2x_0^2 z_0 \gamma_3}{x_\lambda l} \right) \right), \tag{48}$$

$$N = [2x_0\sqrt{y_3}],\tag{49}$$

where $k_{\rm F}$ is the wave vector of a charge carrier with Fermi energy.

In contrast, for a non-degenerate electron gas, the dimensionless conductivity ($\exp u_u \ll 1$) is determined as:

$$\sum = \frac{1}{x_0 z_0 \gamma_1 \sqrt{\gamma_3}} \sqrt{\frac{5}{2\pi}} \sum_{l=1}^{\infty} \exp\left(-\frac{5l^2}{8\gamma_3 x_0^2}\right)$$

$$\times \left(1 - \chi\left(\frac{2x_0^2 \gamma_3 z_0}{x_\lambda l}\right)\right). \tag{50}$$

The further solution of the problem is aimed at finding the relation between the surface wave parameters and the integral conductivity. We calculate the ratio of the electric field intensity vector component E_x to the magnetic field intensity component H_y near the upper boundary of the conducting nanolayer (surface impedance) at the boundary z = 0. Representing the components of the electric and magnetic field intensity vectors as:

$$\begin{cases} E_x = E_{0x}(z) \exp(-i\omega t + ikx), \\ E_z = E_{0z}(z) \exp(-i\omega t + ikx), \\ H_y = H_{0y}(z) \exp(-i\omega t + ikx). \end{cases}$$
 (51)

In this work, the conducting nanolayer is considered to have thickness smaller than the de Broglie wavelength of the charge carriers. In typical metals, the de Broglie wavelength is on the order of the interatomic distance; in typical semiconductors, it is several nanometers, which is significantly smaller than the skin depth. At terahertz frequencies, this depth is on the order of hundreds of nanometers. At terahertz frequencies, this depth is on the order of hundreds of nanometers. From the condition of symmetric distribution of charge carriers at the boundaries of the conducting nanolayer (5), it follows that the *x*-component of the electric field intensity practically does not change across the thickness of the conducting nanolayer.

To find the surface impedance, it is convenient to use the third equation of system (1). Integrating this equation over z, we get

$$H_{y}(a) - H_{y}(0) = -\frac{4\pi}{c} \int_{0}^{a} jdz + i\frac{\omega}{c} E_{x}.$$
 (52)

Taking into account the condition (5) and using the relation between the current density and integral conductivity (21), the expression for the surface impedance takes the form:

$$Z_1 = \frac{E_x}{H_y} \bigg|_{z=0} = \frac{2ic}{(\omega a + 4\pi i\sigma)}.$$
 (53)

Now, we find the surface impedance using the second equation of system (1), which describes the wave behavior in the insulating layer:

$$Z_2 = \frac{E_x}{H_y} \bigg|_{z=0} = -\frac{i\alpha c}{\varepsilon \omega}.$$
 (54)

The components E_x and H_y do not change when crossing the "conductor-dielectric" boundary. Therefore, the surface impedances Z_1 and Z_2 are equal. Equating (54) and (53), we obtain the expression for the transverse decay coefficient of the surface wave:

$$\alpha = -\frac{2\varepsilon\omega}{(\omega a + 4\pi i\sigma)}. (55)$$

By using the relationship (4), we will obtain an expression for the wave vector of the surface wave:

$$k = \sqrt{\frac{\omega^2}{c^2}\varepsilon + \frac{4\varepsilon^2\omega^2}{\omega a + 4\pi i\sigma^2}}.$$
 (56)

We normalize the parameters k and α by the thickness of the conducting nanolayer and write expressions (55) and (56) through dimensionless parameters:

$$\alpha a = -\frac{2\varepsilon y_0}{(y_0 + iy_p^2 \Sigma)},\tag{57}$$

$$ka = \sqrt{y_0^2 \frac{x_0^2}{x_\lambda^2 \rho^2 \varepsilon^2} + \frac{4y_0^2 \varepsilon^2}{(y_0 + iy_p^2 \Sigma)^2}},$$
 (58)

where the following notations are introduced: $\rho = v_{0v}/c$, $y_p = \omega_p \tau_{0v}$.

Conflict of interest

The authors declare that they have no conflict of interest.

References

- [1] S.A. Maier. *Plasmonika: teoriya i prilozheniya* (R&C Dynamics, M., Izhevsk, 2011) (in Russian).
- [2] E. Kretschmann, T.L. Ferrell, C. Ashley. Phys. Rev. Lett., 42, 1312 (1979). DOI: 10.1103/PhysRevLett.42.1312
- [3] G.A. Farias, A.A. Maradudin. Phys. Rev. B, 28 (10), 5675 (1983). DOI: 10.1103/PhysRevB.28.5675
- [4] L.A. Moraga, R. Labbe. Phys. Rev. B, 41, 10221 (1990). DOI: 10.1103/PhysRevB.41.10221
- [5] Zh. Yang, D. Gu, Y. Gao. Opt. Commun., 329, 180 (2014).DOI: 10.1016/j.optcom.2014.05.014
- [6] N. Sharma, A. Joy, A.K. Mishra, R.K. Verma. Opt. Commun., 357, 120 (2015). DOI: 10.1016/j.optcom.2015.08.092
- Zh. Yang, Ch. Liu, Ya. Gao, J. Wang, W. Yang. Chinese Opt. Lett., 14 (4), 042401 (2016).
 DOI: 10.3788/COL201614.042401
- [8] L. Saitta, G. Celano, C. Tosto, F. Arcadio, L. Zeni, C. Sergi, N. Cennamo, G. Cicala. Intern. J. Advanced Manufacturing Technology, 132, 5503 (2024). DOI: 10.1007/s00170-024-13649-x
- [9] H.J. Zhang, Q. Yan, Y.Y. Li, T.R. Zhang, X.L. Zhang, Y.H. Wang, Y.F. Liu. Modern Phys. Lett. B, 37, 33 (2023). DOI: 10.2139/ssrn.4054450
- [10] M.E. Borisova, S.N. Koikov. Fizika dielektrikov (Izd-vo Leningr. un-ta, L., 1979) (in Russian).
- [11] K. Blum. Teoriya matritsy plotnosti i ee prilozheniya (Mir, M., 1983) (in Russian).

- [12] I.A. Kuznetsova, O.V. Savenko, D.N. Romanov. Phys. Lett. A, 427, 127933 (2022). DOI: 10.1016/j.physleta.2022.127933
- [13] M.I. D'yakonov, A.V. Khaetskii. JETP, 55 (5), 917 (1982).
- [14] O.V. Savenko, I.A. Kuznetsova. Proc. SPIE, 12157, 121570W (2022). DOI: 10.1117/12.2622544
- [15] S.B. Soffer. J. Appl. Phys., 38 (4), 1710 (1967).DOI: 10.1063/1.1709746
- [16] A.B. Shmelev. Sov. Phys. Usp., 15, 173 (1972).DOI: 10.1070/PU1972v015n02ABEH004961.
- [17] I.A. Kuznetsova, O.V. Savenko. Semiconductors, 56 (8), 570 (2022).

DOI: 10.21883/SC.2022.08.54116.33.

Translated by J.Savelyeva